

SGCN: Exploiting Compressed-Sparse Features in Deep Graph Convolutional Network Accelerators

Mingi Yoo^{†,1}, Jaeyong Song^{†,1}, Jounghoo Lee[†], Namhyung Kim[‡], Youngsok Kim^{†,*}, and Jinho Lee^{§,*}

[†]Department of Computer Science, Yonsei University

[‡]Samsung Electronics

[§]Department of Electrical and Computer Engineering, Seoul National University

{skys7297, jaeyong.song, jounghoolee}@yonsei.ac.kr, namhyungk11@gmail.com, youngsok@yonsei.ac.kr, leejinho@snu.ac.kr

Abstract—Graph convolutional networks (GCNs) are becoming increasingly popular as they overcome the limited applicability of prior neural networks. One recent trend in GCNs is the use of deep network architectures. As opposed to the traditional GCNs, which only span only around two to five layers deep, modern GCNs now incorporate tens to hundreds of layers with the help of residual connections. From such deep GCNs, we find an important characteristic that they exhibit very high intermediate feature sparsity. This reveals a new opportunity for accelerators to exploit in GCN executions that was previously not present.

In this paper, we propose *SGCN*, a fast and energy-efficient GCN accelerator which fully exploits the sparse intermediate features of modern GCNs. *SGCN* suggests several techniques to achieve significantly higher performance and energy efficiency than the existing accelerators. First, *SGCN* employs a GCN-friendly feature compression format. We focus on reducing the off-chip memory traffic, which often is the bottleneck for GCN executions. Second, we propose microarchitectures for seamlessly handling the compressed feature format. Specifically, we modify the aggregation phase of GCN to process compressed features, and design a combination engine that can output compressed features at no extra memory traffic cost. Third, to better handle locality in the existence of the varying sparsity, *SGCN* employs sparsity-aware cooperation. Sparsity-aware cooperation creates a pattern that exhibits multiple reuse windows, such that the cache can capture diverse sizes of working sets and therefore adapt to the varying level of sparsity. Through a thorough evaluation, we show that *SGCN* achieves $1.66\times$ speedup and 44.1% higher energy efficiency compared to the existing accelerators in geometric mean.

Keywords—Graph Convolutional Networks, Sparsity, Compressed Format, Accelerators

I. INTRODUCTION

Graph convolutional networks (GCNs) are becoming an increasingly popular type of deep neural networks (DNNs) as they can process highly irregular data [37]. They have been successfully adopted to achieve high quality in applications such as node/edge classification [93], molecular structure analysis [16], and classic DNN applications including natural language processing [75] or scene understanding [83].

Even though GCNs fall into a kind of DNN, it is widely known to exhibit a distinct computational characteristic com-

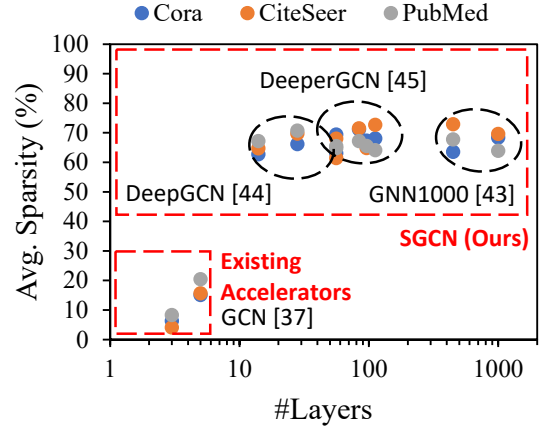


Fig. 1: Average sparsity of intermediate features in traditional and modern GCNs with a various number of layers.

pared to classic DNNs in that they require dedicated accelerator architectures [80], [6], [46], [51], [17], [18], [88], [9], [47]. The early challenge of GCNs has been to deal with the high sparsity of input graph topology. It is known that the graph topology data exhibit near-100% sparsity [41]. Driven by the high topology sparsity, several proposals have been made to take advantage of the hybrid nature in the execution [80], [6], handle load imbalance [51], [17], explore dataflow [47], [88], or reorder the topology [18].

In contrast to the topology data, the per-vertex feature data has often been treated with dense array representation by existing GCN accelerators because the sparsity of the features is far lower than that of the graph topology [17]. Prior efforts targeting the feature accesses were often focused on input features [17] or relied on the fact that the feature width shrinks towards the output layer [17], [46]. Those approaches were attractive with traditional GCNs, especially when the number of layers is small (≤ 5) and each layer width is carefully tuned.

However, recent advances in the GCN are leading to different circumstances. With the introduction of residual connections, modern GCNs [44], [45], [43], [10], [49] now have tens to hundreds, or even a thousand layers, where the feature width remains constant throughout the entire network.

¹Co-first authors.

^{*}Co-corresponding authors.

Fortunately, we make an observation that the modern GCNs exhibit much higher intermediate feature sparsity, providing an excellent opportunity for throughput and energy efficiency. As shown in Fig. 1, the intermediate feature sparsity has been very low in traditional shallow GCNs (up to 20% sparsity). However, with deep GCNs with residual connections [44], [45], [43], the intermediate feature sparsity sharply rises up to 70% as the network becomes deeper. When fully exploited, this intermediate feature sparsity can provide higher performance and energy efficiency. Considering that the majority of the GCN execution is memory-intensive and shows repetitive random accesses, the expected benefit is significant.

There are several key challenges, however, when it comes to fully exploiting the sparsity of the features. First, we need a special format for the GCN intermediate features. Naïvely employing existing sparse formats such as compressed sparse row (CSR) for the features may result in lower performance. Even though CSR is considered a de facto standard for sparse data representation, it is not very efficient for the level of sparsity we observe and the dynamic level of sparsity caused from intermediate features.

Second, existing sparse DNN accelerators do not fit well for handling sparse features of GCNs. There have been several DNN accelerators, often targeting convolutional neural networks (CNNs) [56], [33], [97]. However, their objectives are usually oriented toward reducing the computational workload. Such a strategy could be promising to CNNs because they are computationally intensive, and reducing the number of computations (i.e., MACs) easily translates to performance benefits. However, the computational complexity of GCNs is relatively low, because it usually involves only one MAC operation per each feature element. In such circumstances, the focus should be on reducing the memory traffic volume, not on reducing the amount of computation.

Lastly, the varying level of sparsity makes it difficult to handle locality with tiling techniques. Recent work on GCN acceleration [47], [88] splits the graph topology as well as the feature matrix to reduce the feature working set to fit into cache memory. With such techniques, however, the dynamic level of sparsity cannot be estimated at a static time and makes it difficult to determine the right tile size.

In this paper, we present *SGCN*, a fast and energy-efficient GCN accelerator which minimizes off-chip DRAM accesses by fully exploiting the intermediate feature sparsity of modern GCNs. First, we present *Bitmap-index Embedded In-place CSR* (BEICSR) format that is tailored for GCN execution. Targeting sparsity of roughly around 50%, we find that using bitmaps as indices result in a good compression rate. In addition, by embedding indices in the same row with the content, the accesses can exhibit a much better locality. Furthermore, BEICSR performs an in-place compression because it suits the parallel writes and random reads from GCN execution. Second, we provide microarchitectures and the pipeline structure for executing the sparsity-aware GCNs. We design a sparse aggregator unit that performs the aggregation phase of GCN from features in a compressed format. In addition, we add an

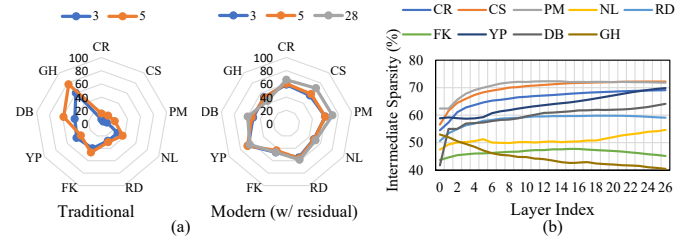


Fig. 2: (a) Effect of residual connection and number of layers on average intermediate feature sparsity and (b) intermediate feature sparsities in layers of modern GCN.

in-place compressor with the ReLU unit in the combination phase, such that the compression can be done without having to pay for extra memory access overhead. Third, we propose sparsity-aware cooperation for handling the varying working set size due to the dynamic level of sparsity. We alter the multiple engines to create access patterns containing various-sized working sets. As a result, even when the working set size is larger than expected, the cache memory can capture a slightly smaller working set that fits into the cache and reuse some portion of the features.

In summary, this paper makes the following contributions:

- We identify the opportunity for utilizing the sparsity of the intermediate features in modern deep GCN execution.
- We present BEICSR, a compressed format designed for sparsity-aware aggregation in GCN executions.
- We present an SGCN accelerator microarchitecture that benefits from sparse feature data in GCN execution.
- We propose sparsity-aware cooperation to handle the varying working set size induced by dynamic levels of sparsity.
- We provide a thorough evaluation for SGCN to show the speedup and energy efficiency gain compared to prior work.

II. MOTIVATION

A. Intermediate Feature Sparsity

In this section, we study the intermediate feature sparsity of deep GCNs. Fig. 2a shows the average feature sparsity of traditional GCNs [37] and modern deep GCNs [45] whose difference is the existence of the residual connections. We chose 3, 5, and 28 layers which are common choices for traditional (3, 5 layers) and modern (28 layers) GCNs.

As previously shown in Fig. 1, traditional GCNs with less than five layers (Fig. 2a-Traditional) show low sparsity, which roughly ranges around 5-30%. Note that 28-layer traditional GCN does not converge for all datasets. On the other hand, with modern deep GCNs (Fig. 2a-Modern), we can make two observations that are distinct from conventional GCNs. First, the addition of residual connection immediately increases the sparsity to a much higher level [66]. As displayed in Fig. 2a-Modern, even in shallow conventional GCNs, adding a residual connection yields over 50% sparsity. When a network is learning well, having around 50% sparsity is normal behavior, and the low sparsity in the traditional GCNs implies that the network struggles to learn a meaningful set of features. Second,

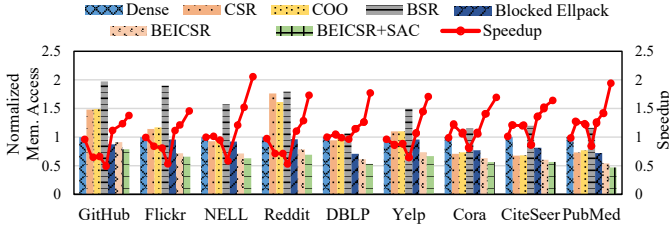


Fig. 3: Comparison of various sparse data representations for GCN intermediate features.

deeper networks have more sparsity in general. Although there are some exceptions, there is a clear trend in Fig. 2a-Modern that deeper networks exhibit higher sparsity. In Fig. 2b, we plot the per-layer sparsity measured from the ‘28 w/ residual’ network. The results reveal that the sparsity varies per dataset, and is generally sparser towards the output layer. This aligns with findings from [63], and can be interpreted as that the network is trying to find disentangled representations [25] for classification tasks.

From the two observations, we found that the higher intermediate feature sparsity exists in modern GCNs across datasets, and is likely to exist in future GCNs too. The goal of SGCN is to utilize this characteristic to design an accelerator with better performance and energy efficiency.

B. Need for a New Accelerator Architecture

In this section, we highlight the need for a new accelerator. The goal is to exploit the ample amount of intermediate feature sparsity for performance benefits. In Fig. 3, we compare the off-chip memory traffic and the performance of GCN accelerators where dense representation, CSR, COO, BSR, Blocked Ellpack and the proposed sparse format (BEICSR) are used for the intermediate features, respectively. We used deep GCNs with 28 layers trained for nine datasets, which exhibit around 40 to 70% sparsity as studied in Section II-A. In the plot, we sorted the datasets in the order of increasing average sparsity for clarity. Please refer to Section VI-A for the detailed setup.

Despite the large potential from the intermediate features, the results show that naïvely supporting sparse features on a GCN accelerator results in little or negative speedup. The colored bars show the number of off-chip memory accesses caused during the execution, and the curves represent the corresponding speedups. From the baseline ‘Dense’ which regards the features as a dense matrix, a naïve approach would be to adopt a CSR data structure for the features as done for sparse graph topology [80], [17], [47], [18], [88] or for CNN intermediate features [57], [2].

Because the GCN executions are known to be highly memory-intensive, the amount of memory traffic is critical to the performance. However, CSR requires an extra element per non-zero value, and fails to provide memory traffic reduction around the provided sparsity range. As a result, the naïve CSR approach experiences a small or negative speedup from the baseline. The COO format has even more index overheads be-

cause it stores both row and column indices for each non-zero element. The problem persists with other sparse formats with block sparsity. Block Compressed Row (BSR) and Blocked Ellpack are popular blocked sparse representations. However, they are beneficial only when there are many empty blocks (e.g., 2×2). Because GCN intermediate activations seldom exhibit such patterns, they are not suitable for GCNs.

On the other hand, the bars denoted ‘BEICSR’ represent our scheme, which utilizes BEICSR for the feature matrix. With an efficient compression format designed for the observed level of sparsity, our scheme successfully converts the sparsity into a reduction in the memory access count. Furthermore, the addition of ‘SAC’ (sparsity-aware cooperation) technique further improves the efficiency of BEICSR. This demonstrates the need for a new accelerator, whose speedup cannot be achieved by existing approaches.

III. BACKGROUND

A. Graph Convolutional Networks

Given a graph topology and a set of incoming features, a conventional graph convolutional network (GCN) produces its outgoing features by performing the operations of its layers on the incoming features. In a basic GCN, the outgoing features of the l -th layer, X^{l+1} , is computed as:

$$X^{l+1} = \sigma(\tilde{A} \cdot X^l \cdot W^l) \quad (1)$$

where σ is a non-linear activation function (e.g., ReLU), often preceded by a normalization function. \tilde{A} is the adjacency matrix of the graph, and X^l and W^l denote the incoming features and weights of the l -th layer, respectively.

In the past, it was believed that GCNs deeper than five layers would lead to very low accuracy, a phenomenon is widely known as over-smoothing [82], [49]. Because of this, the design efforts on GCNs were mostly paid to carefully configuring the feature width of a few layers, usually in a shrinking manner. In this circumstance, one promising approach was to adjust the order of aggregation and combination [17], [47], [46]. Because changing the order of those two phases did not affect the correctness of Eq. (1), the combination was done first on a shrinking layer, and aggregation was done first on an expanding layer to reduce the amount of computation and memory accesses [46]. In addition, sometimes specially handling the first layer was found beneficial [17]. Because the first layer’s input features (i.e., X^1) are not calculated but included in the dataset itself, those can be super-sparse, especially when one-hot encoding is used.

However, as the technology advances, GCNs have evolved to employ residual connections, which alters Eq. (1) to:

$$\begin{aligned} S^{l+1} &= S_{res}^{l+1} + S^l, \\ S_{res}^{l+1} &= \tilde{A} \cdot X^l \cdot W^l, \\ X^l &= \sigma(S^l). \end{aligned} \quad (2)$$

Fig. 4 illustrates the operation. The calculation of $\tilde{A} \cdot X^l$ and its variants are usually called *aggregation*, which does not involve trainable weights. It is the process of collecting

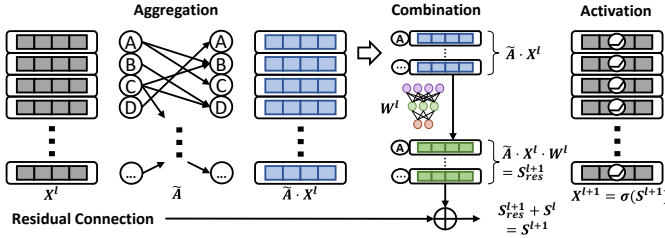


Fig. 4: Operations of a modern GCN layer.

the features from neighboring vertices and aggregating them. The calculation of $X^l \cdot W^l$ and its variants are often called *combination* as it computes the next layer’s features by linearly combining the incoming features and the weight parameters.

With the introduction of residual connections, it was found that GCNs can be as deep as convolutional neural networks, and tens [10], [44], [45] to even a thousand layers [43] are being used for state-of-the-art GCNs. With deep layers, these designs now have uniform feature widths, which invalidates the phase ordering technique. Furthermore, the sparsity of the input features now does not have much impact on the total execution time, as the speedup would be amortized over the tens of layers. Fortunately, this use of residual connections dramatically increases the sparsity of the intermediate features, which enables another opportunity for performance improvement of GCNs.

B. Hardware Acceleration of GCNs

Often, the key to the GCN accelerators is supporting the hybrid nature of aggregation and combined phases. Some architectures implement shared units that support varying datapath for both phases [17], [47], [51], and others implement separate units and pipeline two phases [80], [9], [18], [88].

Table I summarizes the characteristics of the existing GCN accelerators. GCN accelerators can be further classified into two types depending on which of the aggregation and combination phases get performed first. *Aggregation-first* accelerators perform the aggregation phase followed by the combination phase. That is, an aggregation-first accelerator first computes $\tilde{A} \cdot X^l$ followed by $(\tilde{A} \cdot X^l) \cdot W^l$. *Combination-first* accelerators, on the other hand, compute $X^l \cdot W^l$ followed by $\tilde{A} \cdot (X^l \cdot W^l)$. The advantage of each path lies in whether the width of the features increases or decreases after the combination phase, and some approaches suggest utilizing the differences [47], [46]. However, with the introduction of deep GCNs [10], [44], [45], [43], the intermediate feature widths usually remain the same throughout the network, and the differences disappear.

Fig. 5 shows the baseline GCN accelerator architecture, similar to prior art [80], [9], [88], where the green shaded units have been added for SGCN. The aggregation unit uses SIMD MAC cores to process the accumulation of features from multiple vertices. The topology matrix \tilde{A} is assumed to be in a CSR format to employ the high sparsity. Similar to graph processing accelerators [21], [55], [40], a graph reader reads the indices vertex indices and the corresponding

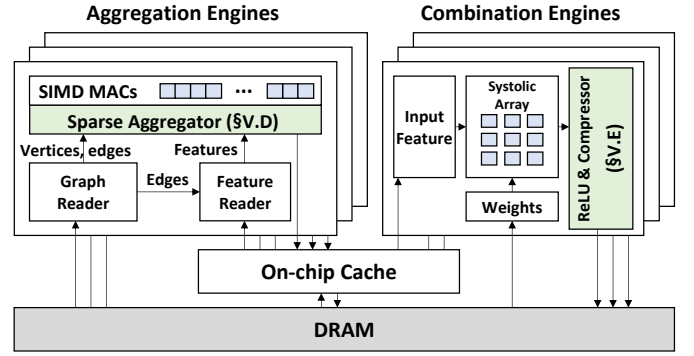


Fig. 5: Our GCN accelerator architecture exploits the high sparsity of graphs. Green modules are added for SGCN.

edges. From the edge information, the feature reader fetches the feature vectors of the edge destinations. Together, these modules feed the SIMD cores to continuously process the aggregation without being stalled. Each module has a small buffer to temporarily store prefetched values to avoid stalls from upstream backpressure.

As accesses to the feature vectors from neighboring vertices exhibit a highly randomized pattern over a wide range of data, a sizable on-chip memory is used as a global cache resembling a last-level cache in modern CPUs. However, the working set size often far exceeds the capacity of the global cache, prohibiting an efficient use of the inherent locality in the feature vector accesses, leaving the aggregation phase highly memory intensive.

The combination engine contains a systolic array for matrix multiplications at its core, similar to conventional DNN accelerators [32], [38]. The input feature and weight buffers provide input matrices, X and W , respectively, to the systolic array. The output is written back to the off-chip DRAM, usually becoming the input to the next layer.

IV. DESIGN GOALS

From the motivation, our objective is to **devise a sparse format** for the features and **design an accelerator microarchitecture** that efficiently process them. For the objective, the following design goals were set in deriving the schemes for SGCN.

First, the primary target should be the memory access reduction, not the computation or the capacity. The primary

TABLE I: Comparison of GCN Accelerators

Accelerator	Compressed Feature?	Target Layers	Residual	Execution Order
AWB-GCN [17]	✗	2	✗	Comb. first
EnGN [51]	✗	2	✗	Comb. first
HyGCN [80]	✗	1-2	✗	Aggr. first
Bidirectional [46]	✗	3	✗	Both
GCNAX [47]	✗	2	✗	Both
I-GCN [18]	✗	2	✗	Comb. first
SGCN (Ours)	✓ BEICSR (§V-A)	>5	✓	Aggr. first

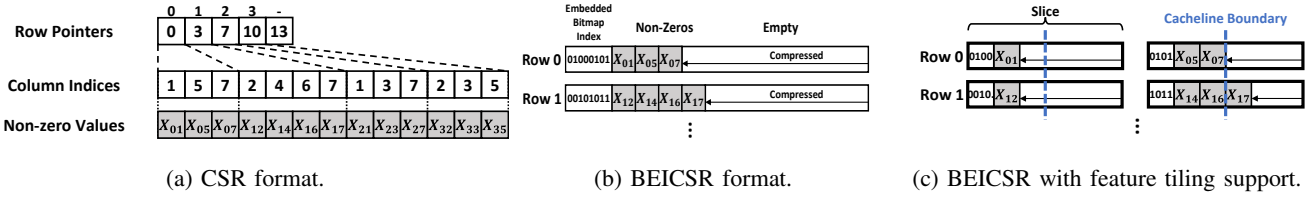


Fig. 6: Compression formats of the feature matrix.

bottleneck of GCN execution is known to be the aggregation phase, which is extremely memory intensive [9], [18]. This indicates that solely optimizing the amount of computation without memory traffic reduction (e.g., zero skipping) would not be an optimal choice.

Second, the format and the resulting access pattern should be cache- and DRAM-friendly. In contrast to CNNs where the feature accesses can be done sequentially, GCN aggregation features incur random accesses of small per-vertex features (i.e., a few cachelines). When dealing with sparse formats, special care must be taken that each access is aligned to the cacheline and/or the DRAM burst length to optimize off-chip traffic. Furthermore, because the intermediate features are dynamically created as a result of the previous layer, the format should allow parallel writes as well as reads. Especially with variable length rows as a result of compression, it is easy for the access pattern to exhibit many unaligned accesses or bank conflicting accesses. Such a problem appears more often for modern memory systems such as HBM that do not support multi-rank channels. Thus, the compression format and its execution should be aware of the memory subsystem and exploit it.

Third, the execution should embrace existing GCN accelerators. For example, existing accelerators employ overlapping between phases [80], [47] or topology/feature tiling [47], [88]. Naïvely applying compressed format and execution flow could potentially disable such techniques, especially with variable sparsity levels that cannot be estimated statically. With the sparsity-aware GCN execution, such techniques must be embraced to achieve maximum performance.

V. SGCN ARCHITECTURE

A. Compression Format

The ultimate purpose of compression from SGCN is to reduce off-chip memory access. This is obviously sensitive to the compression format which we employ for the feature matrix. Compared to the conventional sparse DNN accelerators [56], [33], the difference is that the feature matrix of GCNs exhibit a highly randomized pattern due to the extremely sparse nature of the topology matrix \tilde{A} . For each random access, a portion of a vertex feature array is accessed, which usually spans a few cachelines.

A naïve choice for dealing with sparse data is a compressed sparse row (CSR). However, applying a naïve CSR will not result in off-chip traffic reduction. With CSR, every non-zero element requires two values: one for the column index, and the other for the value itself. Thus, at sparsity below 50%, there

is only capacity overhead instead of reduction, as exemplified in Section II.

To tackle the above issues, we propose BEICSR (Bitmap-index Embedded In-place CSR) format for the intermediate GCN features. Fig. 6 illustrates the conventional CSR format (6a) and the compression format proposed for SGCN (6b) against the same set of data. We make the following design choices for the format:

Embedded Bitmap Index. Instead of column indices, we use *bitmap indices* for each vertex. For example, if an example array of size four is (0, 0.3, 0.5, 0), we place 0110'b followed by the non-zero array (0.3, 0.5). Assuming the feature vector has elements with 50% sparsity, and each element occupies 32 bits, we can calculate the overhead of the bit vector index. when the feature vector width is n , the bitmap index size is n bits, and the non-zero feature data size is $32n \times 0.5 = 16n$. Therefore, it leads to a total index overhead of only 6.25% in that case ($n/16n$), which would be much lower than that of the naïve CSRs that require one integer index per non-zero element. On the other hand, if we use CSR for the same 50% sparsity, we have $32n \times 0.5$ overhead for the column indices plus the row pointers to indicate the starting location of the arrays. Combined with the non-zero feature data size, it would result in an increased size instead of compression.

In addition, we pose to *embed the bitmap index* at the head of the same array which stores the non-zero values. In compressed formats, indices are commonly placed in an independent array. However, such a choice would result in a poor memory access pattern. When a bit vector index for a row is accessed, the surrounding cache line containing indices for other rows is always accessed together in single memory access. Unless reused before eviction, they are considered overhead. Observing the access pattern, the accesses to the bit vector index are almost always followed by the non-zero values. The only exception is when the bit vector index contains all zeros. (i.e., no non-zero element in the row). However, considering that the sparsity is around 50% and each element has little dependence on the other, such an occasion is unlikely. Therefore, the choice of embedding the bitmap index in the same array with the non-zero values yields a better memory access pattern. Note that there exist some formats using bitmap indices [74], [91], but they rely on entirely empty rows [74] or blocks [91] and hence are inappropriate for GCN features.

In-place Compression. A common problem with using compressed formats for performance is the variable lengths. Not only this would necessitate an indirection array similar to

a row pointer, but also result in frequent misaligned memory accesses that lead to traffic volume overhead. To store the offsets for each row, some indirection array equivalent to a row pointer would be needed. Instead, we compress the data row-by-row and store each row at the same reserved place in the memory as if the row was left uncompressed. Even though this would give no benefit to the memory capacity, we argue that such a choice is almost necessary for the following reasons. First, it would provide reduced off-chip traffic aligned to the cacheline boundaries. The alignment is especially important, since the access granularity only spans a few cachelines. Much of the space reserved for a row would be empty, and therefore not accessed from the memory. Furthermore, the beginning of each row can be cacheline-aligned, such that the loss from misalignment can be minimized. Second, it allows parallel writes at the output of each layer. Naively using a variable length storage format requires serialization, because we do not know the size of the compressed feature array from each vertex. Such a choice would incur an intolerable overhead to the execution time. Lastly, because the sizes of the rows are uniform, there is no need for an indirection array. Locating the compressed data just involves a multiplication with the vertex id, which eliminates the need for accessing indirection arrays. This scheme reduces the memory access count and contributes towards row-buffer locality, and achieves better memory bandwidth utilization.

B. Supporting Feature Matrix Slicing

Many modern GCN accelerators propose slicing the feature matrix for better data reuse [87], [88], [47]. When compressing the entire row together, accessing a slice of the feature matrix involves the following sequence: 1) Read the bit vector index to find the range of non-zero values corresponding to the slice, 2) read multiple cachelines that contain non-zero values from the slice, and 3) perform aggregation.

The pitfall from the above sequence is the overhead of unaligned accesses. For example, when there are 16 non-zero values (64 bytes) in a slice, unaligned access would almost always require two 64B cachelines, which neutralizes the benefit from the sparsity.

Therefore, we employ *sliced BEICSR* as depicted in Fig. 6 (c). Instead of a single set of bit vector indices for the entire row, we partition the bit vector and embed it in the head of each corresponding unit slice. Then we align the slices to the burst boundaries. Using the in-place compression from Section V-A for each slice, we allocate the memory space that can hold the maximum number of non-zeros within them (i.e., a dense slice). With the right choice of the unit slice size C , the wasted amount of memory access can be minimized because the number of non-zero elements has a small variance and there are only a few outliers. When a larger slice size is desired, we can simply combine multiple unit slices to form a large logical slice, which incurs almost no difference compared to having a large slice in the first place. In the default design of SGCN, we empirically set $C = 96$, which would occupy 384 bytes in single precision features, and with around 50%

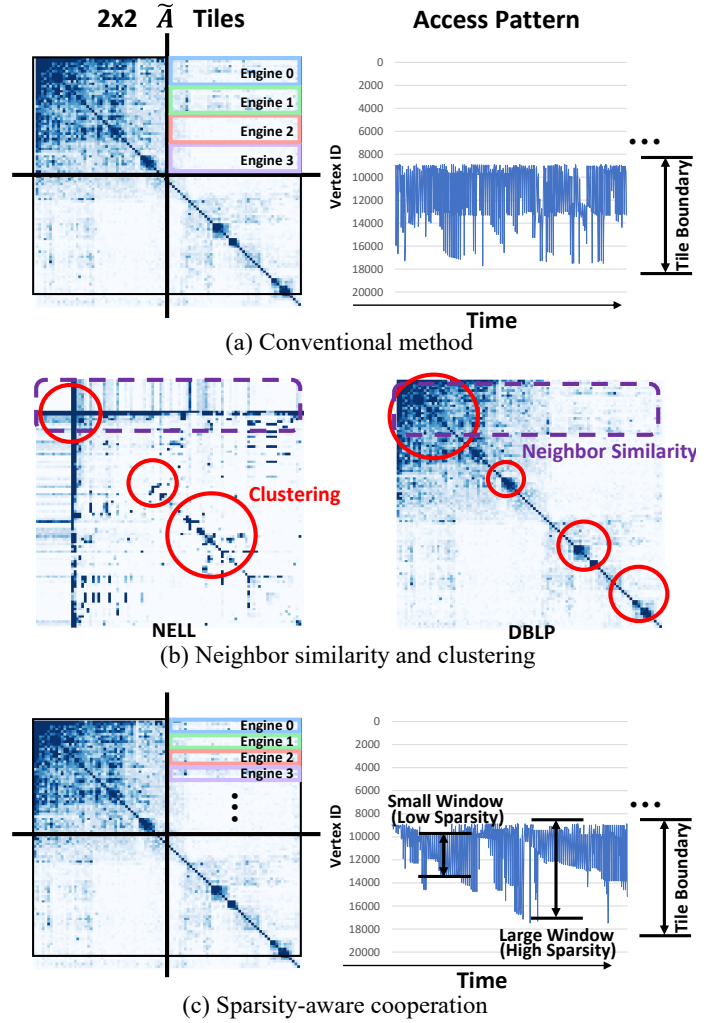


Fig. 7: (a) Conventional method, (b) density heatmap from adjacency matrices of the NELL and DBLP graph, and (c) sparsity-aware cooperation assuming 2×2 tiling.

sparsity it fits into two or three cachelines along with the embedded bitmap indices.

C. Sparsity-Aware Cooperation for Graph Topology Tiling

Another promising technique for GCN execution is graph topology tiling [99], [47], [17]. Partitioning the adjacency matrix into multiple tiles helps reduce the working set size of the intermediate features such that it fits into the cache size. Existing approaches usually find the optimal tile size based on an off-line analysis, often by statically calculating the working set size [88], [47]. However, with SGCN, the level of sparsity varies dynamically depending on each vertex, dataset, and layer. Because of this, estimating the optimal tile size is very difficult, and a working set size exceeding the cache capacity results in significant performance degradation.

Fig. 7a shows how conventional graph tiling works on an example of 2×2 tiling. On the right side, it shows vertex IDs of the features that are accessed for the first 300 reads. When a graph is partitioned into tiles, the working set size is confined

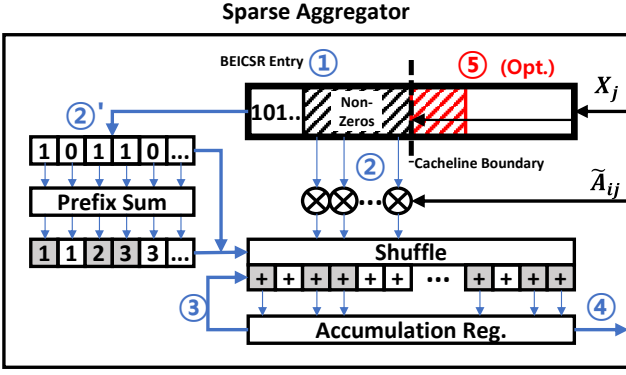


Fig. 8: SGCN sparse aggregator unit microarchitecture.

to the features of the vertices included in a tile, which can fit into the cache. However, when the sparsity of the features is lower than expected, the effective working set size increases because there are more non-zeros per vertex. This has the risk of exceeding the cache capacity, and the performance would quickly drop due to the thrashing pattern [61], [95], [78].

To address this issue, we propose *sparsity-aware cooperation*, a method that alters the access pattern such that there are variously sized working sets that can be captured by the caches. It is known that graphs often form community clusters [19], and there exists a neighbor similarity between adjacent vertices [7]. For example, the example density map from NELL [8] and DBLP [72] displayed in Fig. 7b shows that adjacent rows tend to exhibit the same patterns, and have strong clustering around the diagonals.

Sparsity-aware cooperation takes advantage of this, and each engine accesses a small strip of vertices in an interleaved manner as illustrated in Fig. 7c. For the height of strips, we empirically use 32. Because of the neighbor similarity and clustering, the access distances tend to be shorter, and there are multiple working sets with diverse sizes that can be captured. As a result, when the sparsity level is high, the cache will capture the larger working set window (denoted as ‘large window’), and when the sparsity is low, the cache can capture a smaller working set window to avoid thrashing (denoted as ‘small window’).

D. Sparse Aggregation

Fig. 8 reveals the microarchitecture of the sparse aggregator unit in SGCN and its execution procedure. Each sparse aggregator of SGCN has 16 multipliers, which can process a single cache line worth of data together. ① When a row of the feature matrix X is selected, its first 64 bytes are fetched to the aggregation engine, where its head contains the bitmaps and the rest contains the non-zero values. ② The non-zero values are multiplied with the corresponding edge weight of \tilde{A} broadcasted each multiplier. ③ In parallel, the bitmap is processed by a parallel prefix sum unit to convert the 1’s in the bitmap to a reversed index to the non-zero values. ④ The bitmap and the reversed indices are sent to the accumulator. If the bitmap value is 1, the accumulators at

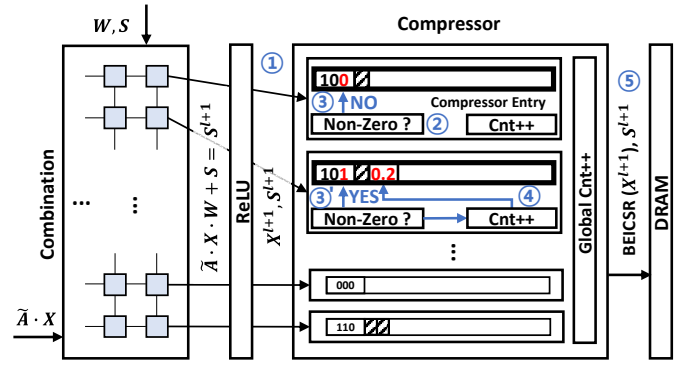


Fig. 9: SGCN compressor unit microarchitecture.

the corresponding positions load the multiplier outputs and add them to the current value. ④ When the accumulation for a single vertex is complete, it is sent to the combination engine for performing combination, ReLU, and compression. ⑤ (Optional) When there are still non-zeros remaining in the next cacheline (identified by the prefix sum result), the next 64 bits are fetched to perform ①-④ again.

E. Post-Combination Compression

Fig. 9 illustrates the compressor unit in SGCN and the compression process. To avoid the extra memory access for the compression, we place the compressor at the output stage of the combination engine using an output-stationary systolic array. One compressor entry containing BEICSR buffer and compression logic is assigned to each row of the systolic array. ① When the combination phase is complete, the data are streamed to the compressor after processing the residual addition and the ReLU activation. ② The compression logic checks whether the output value is zero. ③ If the output value is zero, the bitmap index in the compression entry appends a ‘0’. ④ When the output value is non-zero, the bitmap index accumulates a ‘1’, and ⑤ the output value is saved to the location pointed by the counter. The compressor continuously performs ①-④ for each output value from the systolic array. ⑥ After the compressor has processed a unit slice amount of data, the data stored in the buffer is flushed to the DRAM, and the compressor is re-initialized.

F. Putting It All Together

Fig. 10 presents the overall procedure of SGCN on top of the baseline architecture (Fig. 5). The sparse aggregator unit takes \tilde{A} , the graph topology in CSR format, and X^l in BEICSR format from the output of the previous layer. Similar to [80], [51], [88], we use row-product-based dataflow, and apply tiling for both the graph topology \tilde{A} and feature X^l as in [51], [88], [47]. The resulting $\tilde{A} \cdot X^l$ will be dense, because each row of $\tilde{A} \cdot X^l$ will be a weighted sum of several rows from X^l .

After a block of $\tilde{A} \cdot X^l$ is calculated from the sparse aggregator unit, it will be sent to the systolic-array-based combination engine. The systolic array will multiply $\tilde{A} \cdot X^l$ with W^l , which is essentially a GeMM operation. To perform

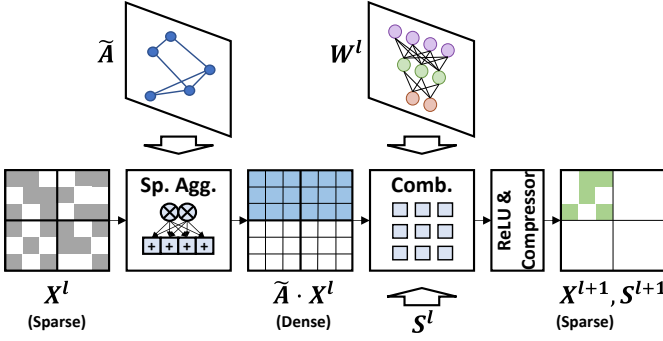


Fig. 10: SGCN execution flow for a GCN layer.

the residual addition, the registers at the systolic arrays are initialized with S^l instead of zero. When a sliced row of $\tilde{A} \cdot X^l \cdot W^l$ is calculated, it is fed to the compressor unit after being activated by ReLU. The output of ReLU activation is the next layer's input feature X^{l+1} . Before being written to the memory, the post-combination compression unit converts the row of X^{l+1} into the BEICSR format. In modern GCN architectures, the input and output feature widths are often the same [10], [43]. In such cases, X' consumes the same capacity with $\tilde{A} \cdot X$, and compressed X' is written in place of $\tilde{A} \cdot X$ to reduce the memory requirement.

Optionally, when the input feature (X^1) is extremely sparse, the combination of the first layer is performed on the sparse aggregator engine instead to take advantage of the sparse input features. Even though this technique only applies to the first layer, this brings a meaningful speedup to some datasets. SGCN does not require much additional implementation cost from the baseline GCN accelerator. For the sparse aggregator units, only the additional prefix sum units are required for reading the bitmap index. For the SGCN compressor units, the global counter and non-zero comparators are added to the basic combination unit to write the bitmap index in addition to the features.

VI. EVALUATION

A. Experimental Setup

We chose nine real-world graph datasets from various sources, listed in Table II. As sparsity of the actual trained model is essential for SGCN, we trained 28-layer GCNs with residual connection and 256 features per vertex by these datasets based on practices of [44], [45].

Cora (CR), CiteSeer (CS), PubMed (PM), DBLP (DB) are citation network graphs from [68], [72]. Each node (document)

TABLE II: Benchmark Dataset Information

Dataset	#Vertices	#Edges	#Input Features	Topology	Feature	Sparsity (w/ 28 layers)	Accuracy (w/ 28 layers)
Cora (CR)	0.003 M	0.01 M	1,433	0.09 MB	0.01 GB	66.1 %	76 %
CiteSeer (CS)	0.003 M	0.009 M	3,703	0.08 MB	0.05 GB	69.7 %	66 %
PubMed (PM)	0.02 M	0.09 M	500	0.75 MB	0.04 GB	70.7 %	77 %
NELL (NL)	0.07 M	0.25 M	61,278	2.17 MB	15.0 GB	51.0 %	64 %
Reddit (RD)	232 M	115 M	602	875 MB	0.52 GB	58.4 %	95 %
Flickr (FK)	0.09 M	0.90 M	500	7.21 MB	0.17 GB	46.5 %	48 %
Yelp (YP)	716 M	14.0 M	300	109 MB	0.80 GB	64.0 %	54 %
DBLP (DB)	0.02 M	0.11 M	1,639	0.87 MB	0.11 GB	59.5 %	86 %
GitHub (GH)	0.04 M	0.58 M	128	4.55 MB	0.02 GB	44.6 %	86 %

TABLE III: System Configuration

Accelerator Engine	Frequency Combination Aggregation	1GHz 32×32 Syst. Array 16-Way SIMD
#Engines	Aggregation Combination	8 8
Global Cache	Capacity Ways Replacement	512KB 16 LRU
Off-chip Memory	Spec. Peak Bandwidth Channels Banks	HBM2 256 GB/s 8 4×4

is linked with others and has a feature vector consisting of bag-of-words. NELL (NL) [8] is a knowledge graph from the Never-Ending Language Learning project. Each node has a one-hot vector of length 61,278. Reddit (RD) [81] is a graph often used for GCN kernel evaluation. Flickr (FK) [42] is an image relationship graph, and each node has the description and properties of an image as features. Yelp (YP) is a social relationship graph that has customer reviewers as nodes and their relationships as a link. For YP, we followed [90] while preprocessing. GitHub (GH) [64] is a code hosting relationship graph. We used original features from these datasets.

We performed the evaluation using the accelerator architecture explained in Section III-B, Section V-D and Section V-E. The system configurations are summarized in Table III. Following [47], we used a 512KB global cache unless otherwise stated. The accelerator runs at 1 GHz. The accelerator has 32×32 systolic array-based combination engines and the sparse aggregation engines from Section V-D, with 32bit fixed points for both features and weights.

We designed the accelerator using Verilog HDL and synthesized it using Synopsys Design Compiler with the 45 nm OpenPDK library and scaled it to 32 nm to match the tech node of the on-chip memory model. For the on-chip caches, we used CACTI 6.5 [73] to estimate the area and power consumption because of the lack of a memory cell library. The baseline chip area of GCNAX is 3.95 mm², and the area of the accelerator with SGCN is 4.05 mm², which has 2.5% overhead on the area, accounting for the increased logic in sparse aggregation and compression engines. We validated that it functioned correctly and drew the area and power consumption values. For comparison, our reproduced AWB-GCN consumed 4.25 mm² due to the complicated logic.

To measure performance, we designed a cycle-accurate simulator written in C++. The model is based on SCALE-Sim [67] for the systolic array used in the combination engine, which we extended with an in-house module for the sparse aggregation engine and compression engine. The execution cycle of the computation modules has been validated with the HDL design at the cycle level. For modeling the DRAM subsystem, we use DRAMsim3 [50] with an HBM2 module.

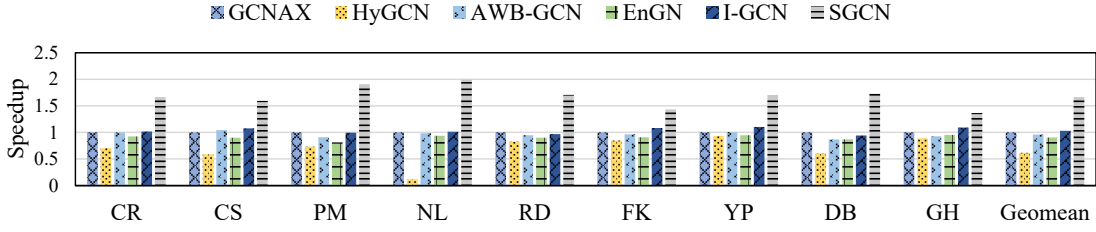


Fig. 11: Performance comparison of GCN accelerators.

B. Fast and Energy-Efficient GCN Executions

Performance. Fig. 11 demonstrates that SGCN outperforms existing GCN accelerators by a great margin. In Fig. 11, the performance of SGCN is compared with the previous methodologies. HyGCN [80] is based on row product execution with hybrid engines. EnGN [51] uses vertex tiling and degree-aware vertex caching (DAVC) to cache high-degree vertices explicitly. AWB-GCN [17] employs column-product-based execution and applies aggressive load-balancing techniques. In addition, I-GCN [18] adopts dynamic reordering to enhance the locality of the graph topology. Moreover, GCNAX [47] is based on perfect tiling and suggests optimized loop ordering based on off-line analysis. Among those, we choose GCNAX as the baseline and report normalized speedups because it shows successful performance over existing accelerators and uses the most similar tiling approach to SGCN.

The results show that SGCN achieves $1.66\times$ speedup over baseline GCNAX in geometric mean, and $2.71\times$ over HyGCN. Because GCNAX employs aggressive tiling for both the topology (\bar{A}) and the intermediate features (X), the speedup of SGCN is mostly from exploiting the feature sparsity. The speedup over HyGCN is mainly coming from two factors: Reduced amount of DRAM accesses due to the usage of BEICSR format, and cache efficiency from graph/feature tiling. Because HyGCN does not perform any tiling/slicing, it suffers from a low cache efficiency for large graphs. AWB-GCN adopts zero skipping on the features, which is a kind of sparsity-aware method. However, AWB-GCN stores the features in a dense format that yields no benefit to the memory traffic. Moreover, it uses the sparsity of the features only in the combination phase which only takes a small portion of the total GCN execution. By adopting a sparse format to reduce the memory traffic, SGCN outperforms AWB-GCN by $1.73\times$ in geometric mean. SGCN also achieves $1.85\times$ speedup compared to EnGN. The degree-aware vertex cache used in EnGN is effective over HyGCN, but its limited vertex tiling still makes lower cache efficiency, so SGCN has an extra advantage over EnGN.

Over the baseline, a large speedup was observed on PubMed and NELL dataset with $1.91\times$ and $1.99\times$ improvement over GCNAX, respectively. The PubMed dataset exhibits high intermediate feature sparsity of almost 70% (see Fig. 2), which translates to a high speedup in the aggregation phase. On the other hand, NELL dataset shows relatively lower feature sparsity. However, its input feature width is exceptionally long (61,278) and is also ultra-sparse (99.9%) because the input

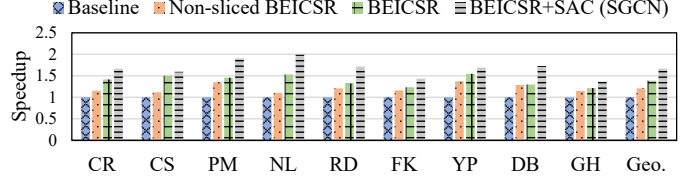


Fig. 12: Ablation study.

features are one-hot encoded vectors. Thus, this unique input layer brings additional speedup, besides the speedup from the intermediate features. On the other hand, speedup numbers from Cora and CiteSeer are similar to the geomean, despite its relatively high sparsity. The reason is partially from the small dataset. When the graph topology is small, the relative portion of the combination phase increases, which amortizes the gain coming from the sparse aggregation. In addition, the average degrees of the two graphs are very low with 3.92 for Cora and 2.76 for CiteSeer where geomean is 10.15 and the maximum is around 500 with Reddit. This means that the number of random accesses to the features is smaller than the other datasets, which also contributes to the amortization of the gain in sparse aggregation.

Ablation Study. Fig. 12 displays how each proposed technique contributes to the performance gain of SGCN. Using GCNAX as the baseline, we first apply the non-sliced version of BEICSR. The non-sliced version of BEICSR is already enough to exploit the intermediate feature sparsity, but settles at suboptimal dataflow due to the lack of feature matrix slicing. As a result, the performance gain is often not large enough. The geometric mean performance gain is 20.8%.

When the feature matrix slicing is supported with the sliced version of BEICSR, sparsity is exploited on the optimal dataflow. The geometric mean speedup is 38.5% from the baseline, which adds 17.7% on top of the non-sliced BEICSR.

Lastly, we add sparsity-aware cooperation to better capture the varying locality of the sparse features. This adds the extra 28.0% speedup in the geometric mean, which results in an overall $1.66\times$ speedup. Sparsity-aware cooperation adds more gain in graphs with more clustered topology (DB) and high neighbor similarity (PM, RD).

Energy Consumption. Fig. 13 shows the advantage of energy consumption. SGCN consumes 44.1% less energy compared to GCNAX, 44.6%, and 58.1% compared to AWB-GCN and HyGCN, respectively. The energy savings come from all three parts of the stack. Much of the energy consumption comes from memory accesses. Because the aggregation phase

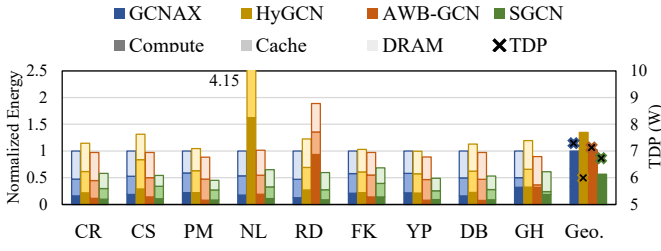


Fig. 13: SGCN energy consumption breakdown.

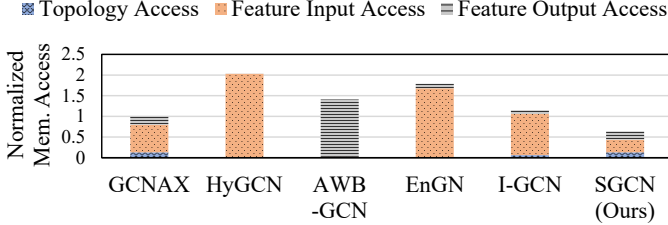


Fig. 14: Off-chip memory access breakdown of Reddit (RD).

requires fewer data due to the sparsity, it affects both the off-chip memory and cache access counts. In addition, the reduced number of multiplications in the aggregation contributes to the energy reduction of the computation. For the peak power, SGCN consumes 6.74W, which is less than AWB-GCN (7.03W) and GCNAX (7.16W). However, it shows higher peak power consumption compared to HyGCN (5.94W) which has slow but simple architecture.

Memory Access Breakdown. Fig. 14 plots the breakdown of the memory accesses during the execution of the RD dataset. In HyGCN, most of the accesses are to the feature. Because it does not use tiling nor utilize the feature sparsity, a lot of duplicate accesses are done to the features which comprise most of the memory access of HyGCN. EnGN reduced some accesses with its degree-aware vertex cache (DAVC). On the other hand, AWB-GCN is based on a column-product dataflow, and it reads each input feature element exactly once. However, the expense is that it requires reading and writing the partial sums more often, which becomes dominating for the memory accesses. GCNAX has balanced memory access with aggressive tiling. I-GCN also shows balanced memory access due to its well-clustered reordering scheme. In contrast, SGCN dramatically reduces the amount of memory access. The main reduction comes from the sparse feature representation, which reduces the feature access by 54.3%.

C. Sensitivity Studies

Number of GCN Layers. In Fig. 15a we plot the geometric averaged performance sensitivity to the number of layers in GCN using CR, CT, and PM datasets. In addition to the default setting of 28 layers, we used 7- to 112-layer GCNs widely used in [44], [45]. In all settings, the sparsity remains mostly constant, and the speedup trend persists. This shows that the performance gain from SGCN is not fine-tuned on a

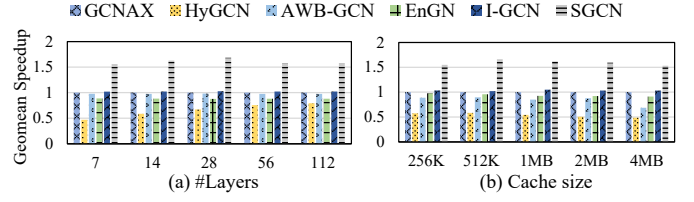


Fig. 15: Sensitivity on the number of layers and cache size.

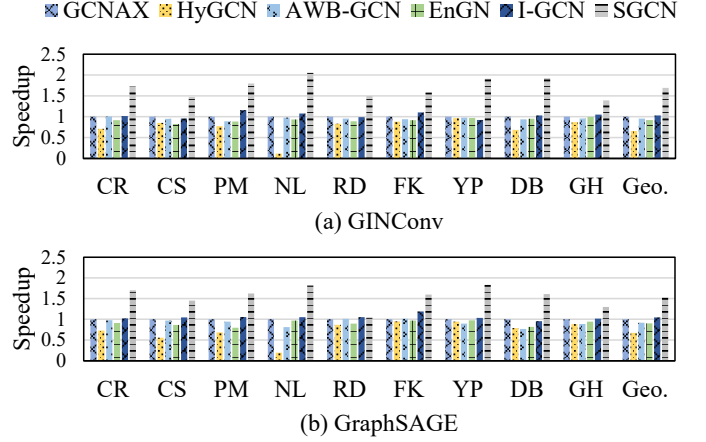


Fig. 16: Performance on (a) GINConv and (b) GraphSAGE.

certain number of layers, and can be broadly used for various specifications.

Cache Size. Fig. 15b plots the trend of a speedup as the cache size increases. In general, the speedup from the sparsity of features is not greatly affected by the cache size unless the data entirely fits into the cache. With a small cache, the benefit of sparsity-aware cooperation becomes marginal because it becomes harder to capture any locality. However, even with larger caches, the speedup remains relatively consistent.

GCN Variants. Fig. 16 depicts the performance result comparison on two additional variants of GCN aggregation: GINConv [79] and GraphSAGE [22]. In both variants, SGCN achieves similar but slightly different speedup from those in Fig. 11. Unlike the GCN aggregation [37], the aggregation phase of GINConv does not require the edge weights. This decreases the size of \tilde{A} , and leads to an increase in the portion of the feature matrix during the aggregation. Because SGCN can efficiently reduce the accesses to the feature matrix, the speedup slightly increases compared to that of the vanilla GCN. On the contrary, GraphSAGE applies random sampling on the edges to reduce the computational overhead. It reduces the effective edge count of the graph topology and reduces the portion of aggregation. Thus, SGCN experiences slightly less, but still significant speedup over the prior arts. In GINConv, SGCN achieves $1.69\times$ speedup over GCNAX and $2.57\times$ against HyGCN. In GraphSAGE, SGCN achieves $1.53\times$ and $2.27\times$ speedup over GCNAX and HyGCN, respectively.

Choice of Slice Size. Another implication of the use of in-place compression with the support for feature matrix slicing is that the speedup can vary depending on the choice of the

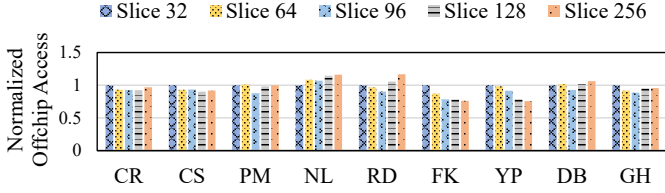


Fig. 17: SGCN slice unit size sensitivity.

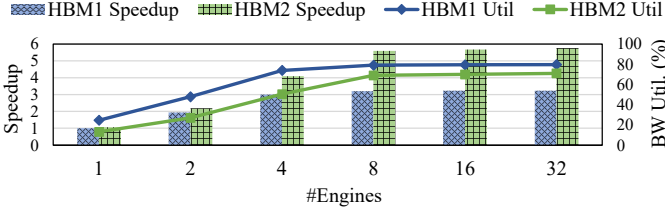


Fig. 18: SGCN memory type and scalability.

unit slice size C . When the slice width is too large, there is a risk of too many slices occupying the extra cache lines. Because this would fetch a lot of invalid data together from the region, it degrades the memory efficiency. On the other hand, if C is too small, the number of slices increases, which affects the amount of output feature accesses. Even though the number of extra cache line access will be small, this could increase the execution time. Nonetheless, Fig. 17 shows that the performance is not very sensitive to the slice size within the range of $C = 32$ to $C = 256$. According to the experiment, the best performance overall is at $C = 96$, but a poor choice still provides a great amount of speedup over the baseline.

Scalability. Fig. 18 shows how SGCN scale with the varying number of engines, with different memory modules (HBM1 and HBM2) used. We distributed the computation to multiple engines. When enough bandwidth is provided, increasing the number of engines provides an almost linear amount of speedup up to around eight engines, demonstrating good scalability. The scalability starts saturating at around 16 engines, which is where the system reaches near the maximum bandwidth of the memory module.

VII. DISCUSSION

A. Range of Sparsity

Based on the observations of Section II, we designed the BEICSR targeting sparsity around 50%. In fact, all the real-world datasets we examined exhibit the intermediate sparsity between 40% and 80%, where we found SGCN to be highly beneficial. Nonetheless, it should be answered which range of sparsity BEICSR has an advantage over the existing techniques. Although highly artificial, we plot the geomean speedup of SGCN over various sparsity levels in Fig. 19. We randomly generated the synthetic input activations of each layer with target sparsity. As displayed, SGCN shows better performance on almost all sparsity ranges. The dense format is better only on sparsity under 5%, because of the additional bitmap indices needed for BEICSR. The break-even point for

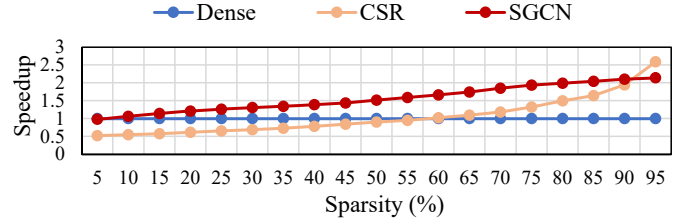


Fig. 19: Performance comparison on various feature sparsity.

CSR is at over 90% sparsity, which is the point where the size of the column indices in CSRs becomes smaller than the bitmap indices of BEICSR.

B. Applicability to Future GCNs

As demonstrated in Fig. 19, SGCN is beneficial over a wide range of sparsity. We would like to argue that the future trend would place the sparsity level in a similar range. The sparsity of activations is caused by the wide use of ReLU functions. With normalized values, the after-ReLU distribution will have a near-zero mean, leading to $\sim 50\%$ sparsity. Therefore, even if GCNs evolve to have distinct characteristics, the sparsity level is unlikely to change towards the extreme levels.

One exception is the input layer, which is often human-designed features. If the input features of the first layer take a one-hot vector format, sparsity can be extremely high as in NELL [8]. In this case, using CSR format for input features can be better, and SGCN performs combination using the aggregation engine which is designed to handle CSR formats. However, the benefit of such a technique is often amortized over tens of layers and hence does not have a significant impact.

VIII. RELATED WORK

A. GCN Accelerators

As GCNs become popular as a critical application domain, the hardware acceleration of GCNs has recently drawn interest from the architecture community. HyGCN [80] claimed the need for GCN accelerators and discussed a few crucial characteristics, such as the hybrid computation pattern and interlayer optimization. Moreover, GNNA [6] proposed a tiled architecture for GCN acceleration based on such hybrid architectures. EnGN [51] discussed the need for tiling the topology and proposed efficient tile ordering using a dedicated cache for high-degree vertices. AWB-GCN [17] proposed using column-based execution and applied several load-balancing techniques. GCNAX [47] is a flexible architecture with an optimal dataflow/buffer configuration found based on perfect tiling. However, perfect tiling overprovisions the required amount of buffer and leads to suboptimal performance. Moreover, the authors assumed a uniform random distribution of the sparse data, which often does not match the actual distribution. SnF [87] addresses the issues of perfect tiling and offline analysis from GCNAX by using a dynamic tiling strategy. By exploiting the repetitive access pattern from

feature tiling, it proposes online dynamic and non-perfect topology tiling. I-GCN [18] suggests a dynamic re-ordering scheme called islandization based on a breadth-first search. In addition, it reuses the overlapping computations within the aggregation phase to reduce the computational complexity. A similar approach has been extended in ReGNN [9], which identifies several redundancies in aggregation and edge updates to further optimize performance. It is also worth noting GCoD [89], which is a co-design approach for GCNs. Similar to pruning approaches for DNNs [39], GCoD prunes, clusters the adjacency matrix, and separately process the dense region and sparse region. However, such methods require retraining of the GCN, and thus can be used when the user can afford the training.

B. Graph Processing Accelerators

Graph processing forms a vital application domain, and many accelerators have been proposed, based on ASICs [21], [55], [86], FPGAs [40], [13], [5], or both [11]. Because of their high bandwidth requirements, graph processing often becomes a primary target for processing-in-memory [1], [92], [100] or processing-in-storage [53], [34]. Tesseract [1] uses the internal bandwidth of HMCs [58] to boost graph processing, which was later refined with better partitioning [92] or execution alignment [100]. GraphSSD is an SSD aware of the graph structures, and GraFboost [34] puts an FPGA accelerator for sort-and-reduce within the storage device for graph processing. However, they primarily target classic graph processing and are not optimized for GCN execution, especially on the sparsity of the per-vertex features.

C. Sparse DNNs

Another stream of related work is on sparse DNN accelerators. Due to pruning and ReLU activation function, many of the weights or the activations become zeros, providing opportunities for optimization. Some prior studies design a computation pruning scheme which is friendly to existing hardware [26], [54], [69]. [98], [76] are extensions to TensorCores that support sparse operations. There are also some designs that eliminate zero-value weights [23], [94], [97], [2], [14] or consider zero-value activations [56], [20], [33], [30]. Some target sparse tensor algebra, targeted to SpMV [65], [4] and SpMM [96], [24], [60]. RingCNN [27] uses ring algebra for algebraic sparsity. In addition, some approaches propose software-hardware co-design of tensor compression [36], [71], [59], [85]. However, these methods primarily target the conventional CNNs, or embedding layers whose characteristics greatly differ from that of GCNs. To the extent of our knowledge, this is the first work on GCN accelerators that proposes techniques for exploiting sparsity in the features.

D. Memory Bandwidth Optimization for DNN Execution

Memories are known to be important factors of DNN accelerators [62], [29], [70], and optimizations focused on memory bandwidth are often crucial to performance. One

popular method is to optimize the on-chip memory usage. Many accelerators adopt different dataflows [15], [12], [32],

and some researchers have claimed that data blocking is more important [84]. In a similar sense, some work has focused on the management of on-chip memories [77], [48], [31]. Another direction is to take advantage of the multi-layered nature of DNNs. By keeping inter-layer data in on-chip memory, the bandwidth for off-chip traffic can be reduced [3], [28], [52], [35]. These methods have been successfully applied to inference [3], [28], training [52], and batch normalization [35]. Among many differences, we highlight that these techniques focus on dealing with on-chip memory management, especially as a manually managed scratchpad. methods are valid because of the highly regular memory access pattern in conventional DNNs and fundamentally different from this work. For GCN execution, irregular accesses from the graphs make it challenging to adopt those common techniques from existing DNN accelerators.

IX. CONCLUSION

We proposed SGCN, a GCN accelerator that exploits the sparsity of intermediate features. With the advance in GCNs towards deep, residual layers, there appears a huge potential from the intermediate feature sparsity that was unavailable from traditional shallow GCNs.

In such circumstances, we present for the first time, exploiting sparsity in the feature data to optimize the memory traffic from the GCN execution. We first identify that a naïve attempt to utilize the feature sparsity could rather result in speed degradation. From the observation, we present BEICSR, a sparse feature representation format designed for the sparse aggregation phase of the GCN execution. In addition, we propose sparsity-aware cooperation, a method for better dealing with the locality in the existence of varying sparsity, with the change in the access patterns. The key ideas of the format are using embedded bitmap indices, in-place compression, and supporting feature slicing technique which is recently used in GCN accelerators. By conducting a thorough evaluation, We demonstrate that SGCN achieves superior performance and energy efficiency compared to the previous state-of-the-art GCN accelerators.

ACKNOWLEDGEMENTS

This work was partly supported by the National Research Foundation of Korea (NRF) grants (2022R1C1C1011307, 2022R1C1C1008131) and Institute of Information & communications Technology Planning & Evaluation (IITP) grants (2021-0-00853, 2020-0-01361) funded by the Korea government (MSIT). The EDA tool was supported by the IC Design Education Center (IDEC), Korea. Mingi Yoo, Jaeyong Song, Jounghoo Lee, and Youngsok Kim were partly supported by the BK21 FOUR (Fostering Outstanding Universities for Research) funded by the Ministry of Education (MOE, Korea) and National Research Foundation of Korea (NRF).

REFERENCES

- [1] J. Ahn, S. Hong, S. Yoo, O. Mutlu, and K. Choi, "A scalable processing-in-memory accelerator for parallel graph processing," in *ISCA*, 2015.
- [2] J. Albericio, P. Judd, T. Hetherington, T. Aamodt, N. E. Jerger, and A. Moshovos, "Cnvlutin: Ineffectual-neuron-free deep neural network computing," in *ISCA*, 2016.
- [3] M. Alwani, H. Chen, M. Ferdman, and P. Milder, "Fused-layer CNN accelerators," in *MICRO*, 2016.
- [4] B. Asgari, R. Hadidi, T. Krishna, H. Kim, and S. Yalamanchili, "ALRESCHA: A lightweight reconfigurable sparse-computation accelerator," in *HPCA*, 2020.
- [5] M. Asiatiki and P. lenne, "Large-scale graph processing on FPGAs with caches for thousands of simultaneous misses," in *ISCA*, 2021.
- [6] A. Auten, M. Tomei, and R. Kumar, "Hardware acceleration of graph neural networks," in *DAC*, 2020.
- [7] P. Boldi and S. Vigna, "The webgraph framework I: Compression techniques," in *WWW*, 2004.
- [8] A. Carlson, J. Betteridge, B. Kisiel, B. Settles, E. R. Hruschka, and T. M. Mitchell, "Toward an architecture for never-ending language learning," in *AAAI*, 2010.
- [9] C. Chen, K. Li, Y. Li, and X. Zou, "ReGNN: A Redundancy-Eliminated Graph Neural Networks Accelerator," in *HPCA*, 2022.
- [10] M. Chen, Z. Wei, Z. Huang, B. Ding, and Y. Li, "Simple and deep graph convolutional networks," in *ICML*, 2020.
- [11] X. Chen, T. Huang, S. Xu, T. Bourgeat, C. Chung, and Arvind, "FlexMiner: A pattern-aware accelerator for graph pattern mining," in *ISCA*, 2021.
- [12] Y.-H. Chen, T. Krishna, J. S. Emer, and V. Sze, "Eyeriss: An energy-efficient reconfigurable accelerator for deep convolutional neural networks," *JSSC*, 2016.
- [13] V. Dadu, S. Liu, and T. Nowatzki, "PolyGraph: Exposing the value of flexibility for graph processing accelerators," in *ISCA*, 2021.
- [14] C. Ding, S. Liao, Y. Wang, Z. Li, N. Liu, Y. Zhuo, C. Wang, X. Qian, Y. Bai, G. Yuan, X. Ma, Y. Zhang, J. Tang, Q. Qiu, X. Lin, and B. Yuan, "CirCNN: Accelerating and compressing deep neural networks using block-circulant weight matrices," in *MICRO*, 2017.
- [15] Z. Du, R. Fasthuber, T. Chen, P. lenne, L. Li, T. Luo, X. Feng, Y. Chen, and O. Temam, "ShiDianNao: Shifting vision processing closer to the sensor," in *ISCA*, 2015.
- [16] A. Fout, J. Byrd, B. Shariat, and A. Ben-Hur, "Protein interface prediction using graph convolutional networks," in *NeurIPS*, 2017.
- [17] T. Geng, A. Li, R. Shi, C. Wu, T. Wang, Y. Li, P. Haghi, A. Tumeo, S. Che, S. Reinhardt, and M. C. Herboldt, "AWB-GCN: A graph convolutional network accelerator with runtime workload rebalancing," in *MICRO*, 2020.
- [18] T. Geng, C. Wu, Y. Zhang, C. Tan, C. Xie, H. You, M. C. Herboldt, Y. Lin, and A. Li, "I-GCN: A Graph Convolutional Network Accelerator with Runtime Locality Enhancement through Islandization," in *MICRO*, 2021.
- [19] M. Girvan and M. E. Newman, "Community structure in social and biological networks," *Proceedings of the national academy of sciences*, 2002.
- [20] A. Gondimalla, N. Chesnut, M. Thottethodi, and T. N. Vijaykumar, "SparTen: A sparse tensor accelerator for convolutional neural networks," in *MICRO*, 2019.
- [21] T. J. Ham, L. Wu, N. Sundaram, N. Satish, and M. Martonosi, "Graphicionado: A high-performance and energy-efficient accelerator for graph analytics," in *MICRO*, 2016.
- [22] W. L. Hamilton, R. Ying, and J. Leskovec, "Inductive representation learning on large graphs," in *NeurIPS*, 2017.
- [23] S. Han, X. Liu, H. Mao, J. Pu, A. Pedram, M. A. Horowitz, and W. J. Dally, "EIE: Efficient inference engine on compressed deep neural network," in *ISCA*, 2016.
- [24] K. Hegde, H. Asghari-Moghaddam, M. Pellauer, N. Crago, A. Jaleel, E. Solomonik, J. Emer, and C. W. Fletcher, "ExTensor: An accelerator for sparse tensor algebra," in *MICRO*, 2019.
- [25] I. Higgins, D. Amos, D. Pfau, S. Racaniere, L. Matthey, D. Rezende, and A. Lerchner, "Towards a definition of disentangled representations," *arXiv preprint*, 2018.
- [26] W. Hua, Y. Zhou, C. D. Sa, Z. Zhang, and G. E. Suh, "Boosting the performance of CNN accelerators with dynamic fine-grained channel gating," in *MICRO*, 2019.
- [27] C.-T. Huang, "RingCNN: Exploiting algebraically-sparse ring tensors for energy-efficient CNN-based computational imaging," in *ISCA*, 2021.
- [28] C.-T. Huang, Y.-C. Ding, H.-C. Wang, C.-W. Weng, K.-P. Lin, L.-W. Wang, and L.-D. Chen, "eCNN: A block-based and highly-parallel CNN accelerator for edge inference," in *MICRO*, 2019.
- [29] B. Hyun, Y. Kwon, Y. Choi, J. Kim, and M. Rhu, "NeuMMU: Architectural support for efficient address translations in NPUs," in *ASPLOS*, 2020.
- [30] J.-W. Jang, S. Lee, D. Kim, H. Park, A. S. Ardestani, Y. Choi, C. Kim, Y. Kim, H. Yu, H. Abdel-Aziz, J.-S. Park, H. Lee, D. Lee, M. W. Kim, H. Jung, H. Nam, D. Lim, S. Lee, J.-H. Song, S. Kwon, J. Hassoun, S. Lim, and C. Choi, "Sparsity-aware and re-configurable NPU architecture for Samsung flagship mobile SoC," in *ISCA*, 2021.
- [31] T. Jin and S. Hong, "Split-CNN: Splitting window-based operations in convolutional neural networks for memory system optimization," in *ASPLOS*, 2019.
- [32] N. P. Jouppi, C. Young, N. Patil, D. Patterson, G. Agrawal, R. Bajwa, S. Bates, S. Bhatia, N. Boden, A. Borchers, R. Boyle, P.-I. Cantin, C. Chao, C. Clark, J. Coriell, M. Daley, M. Dau, J. Dean, B. Gelb, T. V. Ghaemmaghami, R. Gottipati, W. Gulland, R. Hagmann, C. R. Ho, D. Hogberg, J. Hu, R. Hundt, D. Hurt, J. Ibarz, A. Jaffey, A. Jaworski, A. Kaplan, H. Khaitan, D. Killebrew, A. Koch, N. Kumar, S. Lacy, J. Laudon, J. Law, D. Le, C. Leary, Z. Liu, K. Lucke, A. Lundin, G. MacKean, A. Maggiore, M. Mahony, K. Miller, R. Nagarajan, R. Narayanaswami, R. Ni, K. Nix, T. Norrie, M. Omernick, N. Penukonda, A. Phelps, J. Ross, M. Ross, A. Salek, E. Samadiani, C. Severn, G. Sizikov, M. Snellman, J. Souter, D. Steinberg, A. Swing, M. Tan, G. Thorson, B. Tian, H. Toma, E. Tuttle, V. Vasudevan, R. Walter, W. Wang, E. Wilcox, and D. H. Yoon, "In-datacenter performance analysis of a tensor processing unit," in *ISCA*, 2017.
- [33] P. Judd, A. Delmas, S. Sharify, and A. Moshovos, "Cnvlutin²: Ineffectual-activation-and-weight-free deep neural network computing," *arXiv preprint*, 2017.
- [34] S.-W. Jun, A. Wright, S. Zhang, S. Xu, and Arvind, "GraFBoost: Using accelerated flash storage for external graph analytics," in *ISCA*, 2018.
- [35] D. Jung, W. Jung, B. Kim, S. Lee, W. Rhee, and J. H. Ahn, "Restructuring batch normalization to accelerate CNN training," in *SysML*, 2019.
- [36] K. Kanellopoulos, N. Vijaykumar, C. Giannoula, R. Azizi, S. Koppula, N. M. Ghiasi, T. Shahroodi, J. G. Luna, and O. Mutlu, "Smash: Co-designing software compression and hardware-accelerated indexing for efficient sparse matrix operations," in *MICRO*, 2019.
- [37] T. N. Kipf and M. Welling, "Semi-supervised classification with graph convolutional networks," *arXiv preprint*, 2016.
- [38] H. Kwon, A. Samajdar, and T. Krishna, "Maeri: Enabling flexible dataflow mapping over dnn accelerators via reconfigurable interconnects," in *ASPLOS*, 2018.
- [39] Y. LeCun, J. Denker, and S. Solla, "Optimal brain damage," *NIPS*, 1989.
- [40] J. Lee, H. Kim, S. Yoo, K. Choi, H. P. Hofstee, G.-J. Nam, M. R. Nutter, and D. Jasek, "ExtraV: Boosting graph processing near storage with a coherent accelerator," *pVLDB*, 2017.
- [41] J. Leskovec, J. Kleinberg, and C. Faloutsos, "Graphs over time: Densification laws, shrinking diameters and possible explanations," in *KDD*, 2005.
- [42] J. Leskovec and A. Krevl, "SNAP Datasets: Stanford large network dataset collection," <http://snap.stanford.edu/data>, 2014.
- [43] G. Li, M. Müller, B. Ghanem, and V. Koltun, "Training graph neural networks with 1000 layers," in *ICML*, 2021.
- [44] G. Li, M. Muller, A. Thabet, and B. Ghanem, "DeepGCNs: Can GCNs go as deep as CNNs?" in *ICCV*, 2019.
- [45] G. Li, C. Xiong, A. Thabet, and B. Ghanem, "Deepgcgn: All you need to train deeper gcns," *arXiv preprint*, 2020.
- [46] H. Li, M. Yan, X. Yang, L. Deng, W. Li, X. Ye, D. Fan, and Y. Xie, "Hardware acceleration for gcns via bidirectional fusion," *IEEE CAL*, 2021.
- [47] J. Li, A. Louri, A. Karanth, and R. Bunescu, "GCNAX: A flexible and energy-efficient accelerator for graph convolutional neural networks," in *HPCA*, 2021.
- [48] J. Li, G. Yan, W. Lu, S. Jiang, S. Gong, J. Wu, and X. Li, "SmartShuttle: Optimizing off-chip memory accesses for deep learning accelerators," in *DATE*, 2018.
- [49] Q. Li, Z. Han, and X.-M. Wu, "Deeper insights into graph convolutional networks for semi-supervised learning," in *AAAI*, 2018.

- [50] S. Li, Z. Yang, D. Reddy, A. Srivastava, and B. Jacob, "DRAMsim3: A cycle-accurate, thermal-capable DRAM simulator," *IEEE CAL*, 2020.
- [51] S. Liang, Y. Wang, C. Liu, L. He, L. Huawei, D. Xu, and X. Li, "EnGN: A high-throughput and energy-efficient accelerator for large graph neural networks," *TC*, 2020.
- [52] S. Lym, A. Behroozi, W. Wen, G. Li, Y. Kwon, and M. Erez, "Mini-batch serialization: CNN training with inter-layer data reuse," in *SysML*, 2019.
- [53] K. K. Matam, G. Koo, H. Zha, H.-W. Tseng, and M. Annavaram, "GraphSSD: Graph semantics aware SSD," in *ISCA*, 2019.
- [54] W. Niu, X. Ma, S. Lin, S. Wang, X. Qian, X. Lin, Y. Wang, and B. Ren, "PatDNN: Achieving real-time DNN execution on mobile devices with pattern-based weight pruning," in *ASPLOS*, 2020.
- [55] M. M. Ozdal, S. Yesil, T. Kim, A. Ayupov, J. Greth, S. Burns, and O. Ozturk, "Energy efficient architecture for graph analytics accelerators," in *ISCA*, 2016.
- [56] A. Parashar, M. Rhu, A. Mukkara, A. Puglielli, R. Venkatesan, B. Khailany, J. Emer, S. W. Keckler, and W. J. Dally, "SCNN: An accelerator for compressed-sparse convolutional neural networks," in *ISCA*, 2017.
- [57] A. Parashar, M. Rhu, A. Mukkara, A. Puglielli, R. Venkatesan, B. Khailany, J. Emer, S. W. Keckler, and W. J. Dally, "Scnn: An accelerator for compressed-sparse convolutional neural networks," *ISCA*, 2017.
- [58] J. T. Pawlowski, "Hybrid memory cube (HMC)," in *Hot Chips*, 2011.
- [59] L. Pentecost, M. Donato, B. Reagen, U. Gupta, S. Ma, G.-Y. Wei, and D. Brooks, "MaxNVM: Maximizing DNN storage density and inference efficiency with sparse encoding and error mitigation," in *MICRO*, 2019.
- [60] E. Qin, A. Samajdar, H. Kwon, V. Nadella, S. Srinivasan, D. Das, B. Kaul, and T. Krishna, "SIGMA: A sparse and irregular GEMM accelerator with flexible interconnects for DNN training," in *HPCA*, 2020.
- [61] M. K. Qureshi, A. Jaleel, Y. N. Patt, S. C. Steely, and J. Emer, "Adaptive insertion policies for high performance caching," in *ISCA*, 2007.
- [62] M. Rhu, N. Gimelshein, J. Clemons, A. Zulfikar, and S. W. Keckler, "vDNN: Virtualized deep neural networks for scalable, memory-efficient neural network design," in *MICRO*, 2016.
- [63] M. Rhu, M. O'Connor, N. Chatterjee, J. Pool, Y. Kwon, and S. W. Keckler, "Compressing dma engine: Leveraging activation sparsity for training deep neural networks," in *HPCA*, 2018.
- [64] B. Rozemberczki, C. Allen, and R. Sarkar, "Multi-Scale Attributed Node Embedding," *Journal of Complex Networks*, 2021.
- [65] F. Sadi, J. Sweeney, T. M. Low, J. C. Hoe, L. Pileggi, and F. Franchetti, "Efficient SpMV operation for large and highly sparse matrices using scalable multi-way merge parallelization," in *MICRO*, 2019.
- [66] S. Salman and X. Liu, "Sparsity as the implicit gating mechanism for residual blocks," in *IJCNN*, 2019.
- [67] A. Samajdar, Y. Zhu, P. Whatmough, M. Mattina, and T. Krishna, "SCALE-Sim: Systolic CNN accelerator simulator," *arXiv preprint*, 2018.
- [68] P. Sen, G. Namata, M. Bilgic, L. Getoor, B. Galligher, and T. Eliassirad, "Collective classification in network data," *AI magazine*, 2008.
- [69] F. Silfa, G. Dot, J.-M. Arnau, and A. Gonazález, "Neuron-level fuzzy memoization in RNNs," in *MICRO*, 2019.
- [70] K. Siu, D. M. Stuart, M. Mahmoud, and A. Moshovos, "Memory Requirements for Convolutional Neural Network Hardware Accelerators," in *IISWC*, 2018.
- [71] N. Srivastava, H. Jin, S. Smith, H. Rong, D. Albonesi, and Z. Zhang, "Tensaurus: A versatile accelerator for mixed sparse-dense tensor computations," in *HPCA*, 2020.
- [72] J. Tang, J. Zhang, L. Yao, J. Li, L. Zhang, and Z. Su, "Arnetminer: Extraction and mining of academic social networks," in *KDD*, 2008.
- [73] S. Thoziyoor, N. Muralimanohar, J. H. Ahn, and N. P. Jouppi, "CACTI 5.1," 2008-20, HP Labs, Tech. Rep., 2008.
- [74] K. Ueno, T. Suzumura, N. Maruyama, K. Fujisawa, and S. Matsuoka, "Extreme scale breadth-first search on supercomputers," in *Big Data*, 2016.
- [75] Y. Wang, C. Zhang, Z. Xie, C. Guo, Y. Liu, and J. Leng, "Dual-side sparse Tensor Core," in *ISCA*, 2021.
- [76] S. Vashishth, "Neural graph embedding methods for natural language processing," *arXiv preprint*, 2019.
- [77] X. Wei, Y. Liang, and J. Cong, "Overcoming Data Transfer Bottlenecks in FPGA-based DNN Accelerators via Layer Conscious Memory Management," in *DAC*, 2019.
- [78] C.-J. Wu, A. Jaleel, W. Hasenplaugh, M. Martonosi, S. C. Steely Jr, and J. Emer, "SHiP: Signature-based hit predictor for high performance caching," in *MICRO*, 2011.
- [79] K. Xu, W. Hu, J. Leskovec, and S. Jegelka, "How powerful are graph neural networks?" *arXiv preprint*, 2018.
- [80] M. Yan, L. Deng, X. Hu, L. Liang, Y. Feng, X. Ye, Z. Zhang, D. Fan, and Y. Xie, "HyGCN: A gen accelerator with hybrid architecture," in *HPCA*, 2020.
- [81] P. Yanardag and S. Vishwanathan, "Deep graph kernels," in *KDD*, 2015.
- [82] C. Yang, R. Wang, S. Yao, S. Liu, and T. Abdelzaher, "Revisiting over-smoothing in deep gcns," *arXiv preprint*, 2020.
- [83] J. Yang, J. Lu, S. Lee, D. Batra, and D. Parikh, "Graph r-cnn for scene graph generation," in *ECCV*, 2018.
- [84] X. Yang, M. Gao, J. Pu, A. Nayak, Q. Liu, S. E. Bell, J. O. Setter, K. Cao, H. Ha, C. Kozyrakis, and M. Horowitz, "DNN dataflow choice is overrated," *arXiv preprint*, 2018.
- [85] Y. Yang, J. Emer, and D. Sánchez, "SpZip: Architectural support for effective data compression in irregular applications," in *ISCA*, 2021.
- [86] P. Yao, L. Zheng, Z. Zeng, Y. Huang, C. Gui, X. Liao, H. Jin, and J. Xue, "A locality-aware energy-efficient accelerator for graph mining applications," in *MICRO*, 2020.
- [87] M. Yoo, J. Song, H. Lee, J. Lee, N. Kim, Y. Kim, and J. Lee, "Slice-and-Forge: Making Better Use of Caches for Graph Convolutional Network Accelerators," in *PACT*, 2022.
- [88] M. Yoo, J. Song, J. Lee, N. Kim, Y. Kim, and J. Lee, "Making a Better Use of Caches for GCN Accelerators with Feature Slicing and Automatic Tile Morphing," *IEEE CAL*, 2021.
- [89] H. You, T. Geng, Y. Zhang, A. Li, and Y. Lin, "Gcod: Graph convolutional network acceleration via dedicated algorithm and accelerator co-design," *arXiv preprint*, 2021.
- [90] H. Zeng, H. Zhou, A. Srivastava, R. Kannan, and V. Prasanna, "GraphSAINT: Graph sampling based inductive learning method," in *ICLR*, 2020.
- [91] J. Zhang and L. Gruenwald, "Regularizing irregularity: Bitmap-based and portable sparse matrix multiplication for graph data on gpus," in *GRADES-NDA*, 2018.
- [92] M. Zhang, Y. Zhuo, C. Wang, M. Gao, Y. Wu, K. Chen, C. Kozyrakis, and X. Qian, "GraphP: Reducing communication for PIM-based graph processing with efficient data partition," in *HPCA*, 2018.
- [93] M. Zhang and Y. Chen, "Link prediction based on graph neural networks," in *NeurIPS*, 2018.
- [94] S. Zhang, Z. Du, L. Zhang, H. Lan, S. Liu, L. Li, Q. Guo, T. Chen, and Y. Chen, "Cambricon-X: An accelerator for sparse neural networks," in *MICRO*, 2016.
- [95] X. Zhang, C. Li, H. Wang, and D. Wang, "A cache replacement policy using adaptive insertion and re-reference prediction," in *ISCA*, 2010.
- [96] Z. Zhang, H. Wang, S. Han, and W. J. Dally, "SpArch: Efficient architecture for sparse matrix multiplication," in *HPCA*, 2020.
- [97] X. Zhou, Z. Du, Q. Guo, S. Liu, C. Liu, C. Wang, X. Zhou, L. Li, T. Chen, and Y. Chen, "Cambricon-S: Addressing irregularity in sparse neural networks through a cooperative software/hardware approach," in *MICRO*, 2018.
- [98] M. Zhu, T. Zhang, Z. Gu, and Y. Xie, "Sparse Tensor Core: Algorithm and hardware co-design for vector-wise sparse neural networks on modern GPUs," in *MICRO*, 2019.
- [99] X. Zhu, W. Han, and W. Chen, "GridGraph: Large-scale graph processing on a single machine using 2-level hierarchical partitioning," in *USENIX ATC*, 2015.
- [100] Y. Zhuo, C. Wang, M. Zhang, R. Wang, D. Niu, Y. Wang, and X. Qian, "GraphQ: Scalable PIM-based graph processing," in *MICRO*, 2019.